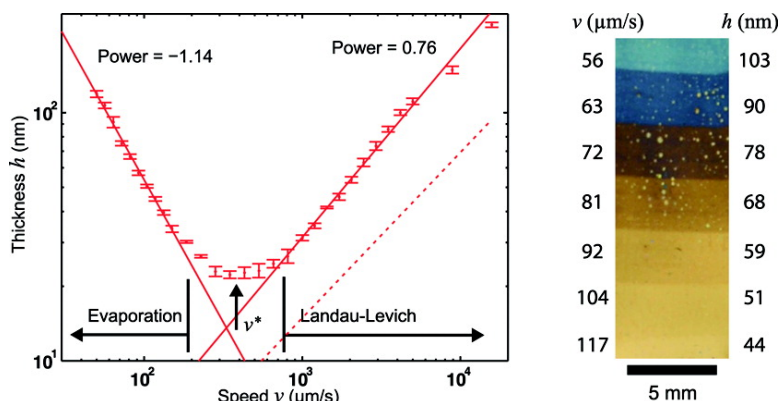


From Convective Assembly to Landau-Levich Deposition of Multilayered Phospholipid Films of Controlled Thickness

Mael Le Berre, Yong Chen, and Damien Baigl

Langmuir, 2009, 25 (5), 2554-2557 • DOI: 10.1021/la803646e • Publication Date (Web): 03 February 2009

Downloaded from <http://pubs.acs.org> on February 24, 2009



More About This Article

Additional resources and features associated with this article are available within the HTML version:

- Supporting Information
- Access to high resolution figures
- Links to articles and content related to this article
- Copyright permission to reproduce figures and/or text from this article

[View the Full Text HTML](#)

From Convective Assembly to Landau–Levich Deposition of Multilayered Phospholipid Films of Controlled Thickness

Maël Le Berre, Yong Chen, and Damien Baigl*

Department of Chemistry, Ecole Normale Supérieure, 24 rue Lhomond, 75005 Paris, France

Received November 3, 2008. Revised Manuscript Received January 12, 2009

In this letter, we describe a method to control the organization and thickness of multilayered phospholipid films. The meniscus of an organic solution of phospholipid molecules was dragged at a speed v on a solid substrate under controlled temperature and forced convection, leading to the deposition of a dried multilayered phospholipid film with a thickness h in the range of 20–200 nm. We found two distinct regimes dominating the film deposition. At low speeds, phospholipid molecules accumulate near the contact line and form a dry film behind the meniscus (evaporation regime). At high speed, viscous forces become predominant and pull out a liquid film that will dry afterward (Landau–Levich regime). Both regimes show robust scaling $h \propto v^\alpha$ with $\alpha = -1.1$ and 0.76, respectively. Although these regimes have been observed separately in the past, they have not been demonstrated in the same material system. Moreover, we present models whose scalings ($\alpha = -1$ and $2/3$) are in close agreement with the observed values. The microscale organization of the resulting film is independent of v for a given regime but differs from one regime to another. In the Landau–Levich regime, h is very homogeneous on the microscale with discrete variations of ± 5 nm, that is, the thickness of one bilayer.

Introduction

The deposition of thin films on solid substrates is of considerable fundamental and practical importance in numerous domains such as microelectronics, optics, and sensors.¹ Various methods, such as chemical vapor deposition (CVD), molecular beam epitaxy (MBE), spin coating, and dip coating, have been developed to obtain a controlled deposition for both laboratory and industrial applications. However, molecules with self-organization properties such as phospholipids (main component of biological membranes) remain difficult to deposit in a controlled way. Although there are well-established techniques for depositing a single phospholipid bilayer on a solid substrate,^{2,3} it remains very difficult to control the thickness and organization of phospholipid multilayer films.^{4–6} In this letter, we introduce the method of the receding meniscus⁷ to deposit multilayered phospholipid films with controlled thickness on a solid substrate. The phenomenon was investigated both theoretically and experimentally. Two regimes were identified depending on the relative importance of evaporation and viscous forces. We analyzed the film properties (thickness, homogeneity, and morphology) on nano-, micro-, and macroscale as a function of the receding speed and deposition regime.

Materials and Methods

Materials. The 100 boron-doped silicon wafers were from Siltronic (Archamps, France). 1,2-Dioleoyl-*sn*-glycero-3-phosphocholine (DOPC) was from Avanti Polar Lipids. 1-Oleoyl-2-[12-[(7-nitro-2-1,3-benzoxadiazol-4-yl)amino]dodecanoyl]-*sn*-glycero-3-phosphocholine (NBD-PC) and all other chemicals were from Sigma.

* Corresponding author. Phone: +33 1 4432 2431. Fax: +33 1 4432 2402. E-mail: damien.baigl@ens.fr.

(1) Madou, M. *Fundamentals of Microfabrication*; CRC Press: Boca Raton, FL, 1997.

(2) Sackmann, E. *Science* **1996**, *271*, 43–48.

(3) Castellana, E. T.; Cremer, P. S. *Surf. Sci. Rep.* **2006**, *61*, 429–444.

(4) Seul, M.; Sammon, J. *Thin Solid Films* **1990**, *185*, 287–305.

(5) Spangenberg, T.; de Mello, N. F.; Creczynski-Pasa, T. B.; Pasa, A. A.; Niehus, H. *Phys. Status Solidi A* **2004**, *201*, 857–860.

(6) Estes, D. J.; Mayer, M. *Colloids Surf., B* **2005**, *42*, 115–123.

(7) Yabu, H.; Shimomura, M. *Adv. Funct. Mater.* **2005**, *15*, 575–581.

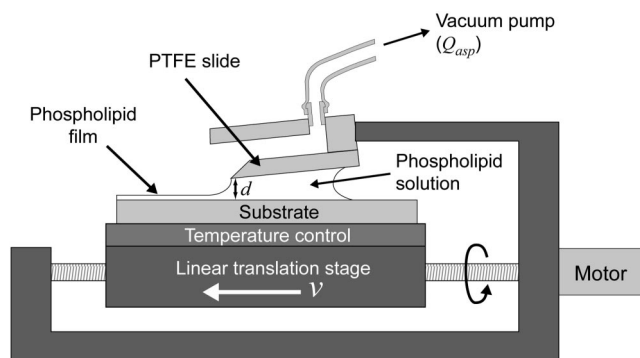


Figure 1. Experimental setup for film deposition (not drawn to scale). v , d , and Q_{asp} are the receding speed, the meniscus height, and the aspiration flow rate, respectively. See the Materials and Methods section for details.

Film Deposition. Figure 1 shows the experimental setup for film deposition. A droplet of a phospholipid solution was dragged on a substrate at constant speed v under controlled temperature and forced convection. A clean silicon wafer, used as the substrate, was mounted on a computer-controlled linear translation stage (M-403.6 PD, PI) equipped with a thermoelectric module for temperature control. The droplet was held by a poly(tetrafluoroethylene) (PTFE) slide (2 cm width) with a sharp end above which air was pumped at a controlled flow rate of Q_{asp} . The droplet holder was micromanipulated to get a well-defined meniscus of height d and a constant tilt angle in the direction of stage displacement. Right after the introduction of a 40 μ L droplet of phospholipid solution between the substrate and the PTFE slide, predeposition on a length of 7 mm at a speed of $v = 1$ mm/s was performed prior to the deposition at the desired speed. All experiments have been performed at 27 °C with a phospholipid solution composed of 98 wt % DOPC and 2 wt % NBD-PC (fluorescent probe) dissolved in *n*-octane at a concentration of 20 mg/mL for all experiments except for the green points in Figure 3A (12 mg/mL).

Ellipsometry. The thickness of dried phospholipid films on silicon was measured by ellipsometry in air using a Sentech SE 400 apparatus. The light source was a helium–neon laser ($\lambda = 632.8$ nm), and the angle of incidence was set to 72°. The thickness was determined using a multilayer model and a refractive index of 1.45 for the

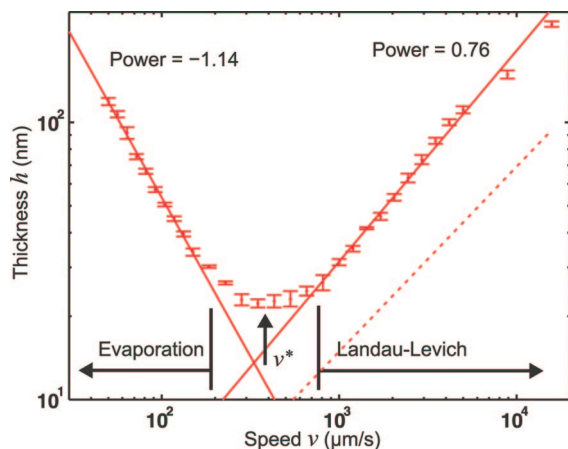


Figure 2. Measured film thickness h as a function of deposition speed v . Two regimes are identified as a function of v : evaporation and Landau–Levich. The solid lines are exponential fits. The dashed line corresponds to the theoretical prediction given by eq 4.

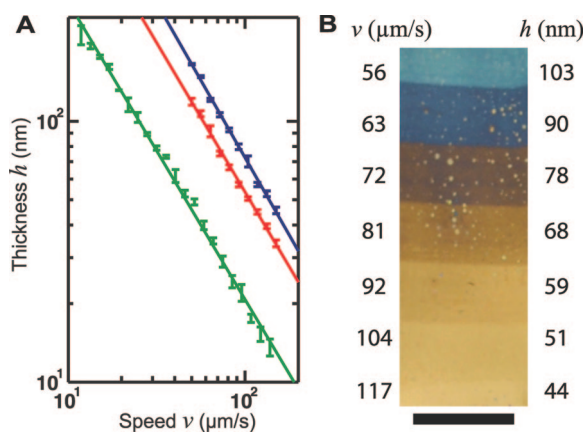


Figure 3. (A) Film thickness h as a function of deposition speed v for different values of meniscus height d (0.75, 0.75, and 0.3 mm) and aspiration flow ($Q_{\text{asp}} = 0.5, 3.5, 0.5$ sccs) (red, blue, and green, respectively). Bars correspond to experimental data (mean \pm SD, $n = 10$). Solid lines are exponential fits providing the parameters shown in Table 1. (B) Photograph in real colors of a phospholipid film deposited on a silicon wafer as a function of speed increasing in a stepwise manner. The speed deposition v and film thickness h measured by ellipsometry are indicated on the left and right of the photograph, respectively. The scale bar is 5 mm.

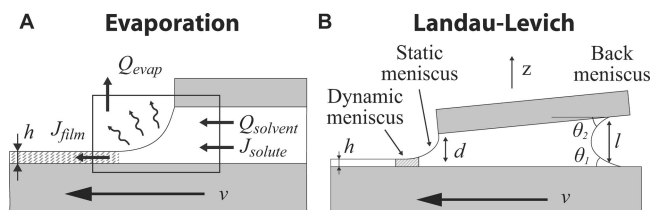


Figure 4. Schematic of the two deposition regimes with parameters used in this work.

phospholipid film. For each film, the measurement was repeated on 10 different locations.

Fluorescence Microscopy. Dried films of phospholipid deposited on silicon were observed by epifluorescence microscopy using an inverted microscope (Aixoobserver D1, Carl Zeiss) equipped with an EM-CCD camera (Photonmax 512B, Princeton Scientific). Fluorescence images were converted to thickness maps (Figure 5) by using a calibration curve linking the average fluorescence to the average thickness measured by ellipsometry (Figure S1 in Supporting Informations).

Table 1. Parameters α (Exponent of v) and Q_{evap}/L (Evaporation Flow Rate per Unit Length) Determined by Fitting Experimental Data (Figure 3A) for Different Values of Meniscus Height d and Aspiration Flow Q_{asp}

d (mm)	Q_{asp} (sccs)	α	Q_{evap}/L ($\mu\text{m}^2/\text{s}$)
0.75	0.5	−1.14	273
0.75	3.5	−1.18	372
0.3	0.5	−1.14	128

Photograph. The picture shown in Figure 3B is a photograph in real colors taken with a Nikon D200 digital camera under ambient light.

Results and Discussions

First, a phospholipid film was deposited using the setup shown in Figure 1 at various receding speeds v and constant meniscus height ($d = 0.75$ mm) and forced convection ($Q_{\text{asp}} = 0.5$ sccs). Interestingly, Figure 2 shows that h as a function of v presents a minimum at a speed of v^* . For $v < v^*$, a film of phospholipid is deposited behind the meniscus. For $v > v^*$, a liquid film is drawn by the substrate, forming a phospholipid film after evaporation of the solvent. We found that v varies as $h \propto v^{-1.1}$ and $h \propto v^{0.76}$ for $v < v^*$ and $v > v^*$, respectively. Figure 3A shows that for $v < v^*$ the same dependency is observed ($h \propto v^\alpha$ with $\alpha \approx -1.1$) regardless of the experimental conditions. However, the prefactor increases with an increase in the forced convection (blue points) and decreases for a lower meniscus height and a lower concentration (green points). For all conditions shown here, the film thickness is homogeneous on the macroscale level ($\pm 3\%$ according to our ellipsometry measurements). All of these results show that the film thickness can be controlled with good precision between approximately 20 and 200 nm by a simple change in the receding speed v . This is illustrated by the picture in Figure 3B showing a real color photograph of a film deposited on a substrate with a speed increasing in a stepwise manner. The experimental results show two regimes of film deposition. This can be interpreted by the relative importance of two phenomena. At low speed, phospholipid molecules are concentrated near the contact line because of solvent evaporation at the meniscus surface (evaporation regime). At higher speed, a liquid film is dragged out by viscous forces and dries afterward (Landau–Levich regime).

The evaporation regime has been previously observed during the drying of sessile droplets and is responsible for the formation of the so-called coffee rings.⁸ This regime of deposition usually named “convective assembly” was mainly applied to organize colloids⁹ and, to a lesser extent, nonvolatile molecules on a solid substrate.^{7,10} Very few theoretical models have been proposed to describe the thickness dependences of the film. On the basis of a microscopic model, Berteloot et al. predicted a thickness of $h \propto v^{-2}$.¹¹ Here, we propose a model based on a simple mass balance in a box surrounding the meniscus (Figure 4A). At steady state, the flow rate of solvent leaving the box by evaporation (Q_{evap}) equals that of solvent molecules entering the box (Q_{solvent}). The conservation of mass imposes that the outward mass flux of phospholipid molecules in the film J_{film} compensates for the inward flux in solution ($J_{\text{solute}} = CQ_{\text{solvent}}$), where C is the bulk phospholipid mass concentration. This leads to

$$h = \frac{C Q_{\text{evap}}}{\rho L} v^{-1} \quad (1)$$

where ρ and L are the density and the width of the phospholipid film, respectively. In this model, the exponent on v is in good agreement with our experimental data ($\alpha \approx -1.1$). Moreover, the estimation of Q_{evap}/L by fitting our data with eq. 1 (Figure

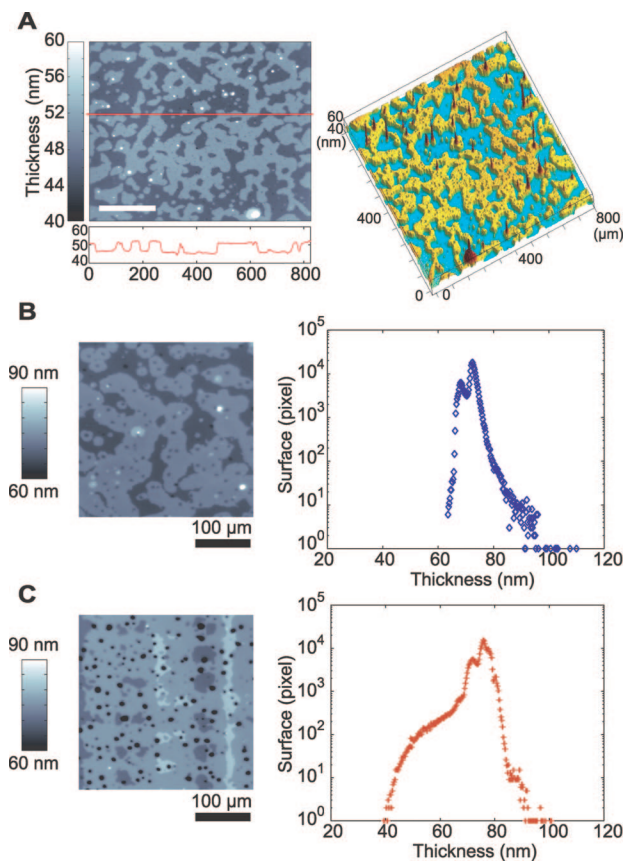


Figure 5. Micro- and nanoscale organizations of the deposited films. (A) (Left) Typical thickness map of a phospholipid film obtained at $v = 1710 \mu\text{m/s}$. The thickness profile below the map corresponds to the solid red line. (Right) The 3D representation. The scale bar is $200 \mu\text{m}$. (B, C) Thickness map (left) and distribution of thicknesses (right) for two films having similar average thicknesses obtained from Landau–Levich (B, $v = 2924 \mu\text{m/s}$; $h = 72 \pm 2.5 \text{ nm}$) and evaporation (C, $v = 81 \mu\text{m/s}$; $h = 74 \pm 4.5 \text{ nm}$) regimes, respectively.

3A) shows that Q_{evap}/L follows the expected evolution when varying d and Q_{asp} (Table 1). The good agreement between this model and the experimental data indicates that the mass balance may be respected in the meniscus; that is, there is no concentrated solution going back to the bulk liquid. This is in contradiction to the theoretical microscopic analysis by Berteloot et al., which predicts a stagnation point inside the meniscus.¹¹ Although this description might be applied to colloidal solutions,¹² special attention has to be paid to noncolloidal solutes, where solutal Marangoni effects have to be taken into account. In this case, the additional flow at the surface of the meniscus¹³ might favor the transport of the concentrated solution toward the contact line. This assumption is supported by two observations: (i) the deposited thickness increases with the height of the meniscus, indicating that the whole meniscus participates in the deposition of matter, and (ii) by adding particles to the droplet, Marangoni flow was observed in the direction of the contact line.

(8) Deegan, R. D.; Bakajin, O.; Dupont, T. F.; Huber, G.; Nagel, S. R.; Witten, T. A. *Nature* **1997**, *389*, 827–829.

(9) Kraus, T.; Malaquin, L.; Schmid, H.; Riess, W.; Spencer, N. D.; Wolf, H. *Nat. Nanotechnol.* **2007**, *2*, 570–576.

(10) Brinker, C. J.; Lu, Y.; Sellinger, A.; Fan, H. *Adv. Mater.* **1999**, *11*, 579–585.

(11) Berteloot, G.; Pham, C.-T.; Daerr, A.; Lequeux, F.; Limat, L. *Europhys. Lett.* **2008**, *83*, 14003.

(12) Deegan, R. D.; Bakajin, O.; Dupont, T. F.; Huber, G.; Nagel, S. R.; Witten, T. A. *Phys. Rev. E* **2000**, *62*, 756–765.

(13) Fanton, X.; Cazabat, A.-M. *Langmuir* **1998**, *14*, 2554–2561.

At high speed ($v > v^*$), viscous forces become strong enough to drag out a liquid film from the meniscus. This well-known phenomenon was described for the first time by Landau, Levich, and Derjaguin¹⁴ and it was detailed afterward in other geometries.¹⁵ In the original Landau–Levich problem, a plate is vertically taken out from a liquid at a constant speed v , and the liquid film thickness h_{LL} equals

$$h_{\text{LL}} = 0.94\kappa^{-1}Ca^{2/3} \quad (2)$$

where $\kappa^{-1} = \gamma/\rho g^{1/2}$ is the capillary length (with ρ and γ being the surface tension and density of the liquid, respectively) and $Ca = \eta v/\gamma$ is the capillary number (with η being the liquid viscosity). In our case, the solid substrate is horizontal, and the liquid is retained by the capillary pressure instead of gravity. In this situation, the curvature $C(z)$ equals

$$C(z) = \frac{l}{2\kappa^{-2}} - \frac{\cos\theta_1 + \cos\theta_2}{l} - \frac{z}{2\kappa^{-2}} \quad (3)$$

where θ_1 , θ_2 , and l are the geometric parameters defined in Figure 4B. By using this expression in the calculation of the dynamic meniscus, we obtained the expression of h for a confined meniscus:

$$h = 1.34 \frac{C}{\rho} \frac{l}{\cos\theta_1 + \cos\theta_2 - \frac{l^2}{2\kappa^{-2}}} Ca^{2/3} \quad (4)$$

The Landau–Levich regime dominates when the amount of solvent dragged by the substrate is larger than the amount of evaporated solvent, that is, when

$$v > v^* = \left(0.75 \frac{l}{\cos\theta_1 + \cos\theta_2 - \frac{l^2}{2\kappa^{-2}}} \frac{\eta^{2/3}}{\gamma^{2/3} \frac{Q_{\text{evap}}}{L}} \right)^{-3/5} \quad (5)$$

In this calculation, we used the back meniscus as the origin of the pressure in the droplet whereas the front meniscus is not constrained because of the sharp end geometry of the slide. The curve corresponding to eq 4 is drawn in Figure 2 as a dashed line. There is good agreement for the power of v (experimentally, $h \propto v^{0.76}$), but a significant difference is observed for the prefactor, which is approximately 2.3 times higher in the experiments. This increased amount of deposited film may be due to solutal Marangoni flow in the droplet driven by the surface tension gradient toward the front meniscus due to evaporation.¹³ In the case of surfactant in water, this effect is known to induce a thickening factor in the range of 1–2.5.¹⁶

Figure 5 shows the microscale organization of films obtained from Landau–Levich and evaporation regimes. For both regimes, we observed a stratified organization with a characteristic step size of $5 \pm 1 \text{ nm}$, which corresponds to the thickness of one bilayer on average (Figure 5A). This is in agreement with observations made with other techniques such as atomic force microscopy⁵ and reflection microscopy,¹⁷ and it indicates that the deposited films are organized in a multilayered fashion on the silicon substrate.⁴ Interestingly, in most cases the height variation in one image ($800 \mu\text{m} \times 600 \mu\text{m}$) does not exceed one bilayer, which demonstrates good homogeneity of the film on the microscale level. However, each deposition regime presents a specific organization (Figures 5B–C). Regardless of v , films obtained by Landau–Levich deposition present large areas of

(14) Landau, L.; Levich, B. *Acta Phys. Chim. U.R.S.S.* **1942**, *17*, 42–54.

(15) Quéré, D.; de Ryck, A. *Ann. Phys. Fr.* **1998**, *23*, 1–149.

(16) Ramdane, O. O.; Quéré, D. *Langmuir* **1997**, *13*, 2911–2916.

(17) Le Berre, M.; Yamada, A.; Reck, L.; Chen, Y.; Baigl, D. *Langmuir* **2008**, *24*, 2643–2649.

homogeneous thickness with a few defects of larger thickness (white spots). In contrast, films obtained by evaporation are composed of smaller domains and contain many small defects of lower thickness (dark spots). To quantify the microscale organization, we established the distribution of thicknesses in both regimes for the same average thickness (Figures 5B–C, right). Both distributions show two strong maxima (the vertical axis is shown on a logarithmic scale) around the average film thickness that are separated by 5 nm (one bilayer). In the evaporation regime, a significant proportion of smaller thicknesses is observed and corresponds to holelike defects in the film (Figure 5C). In contrast, the film obtained in the Landau–Levich regime has a much sharper distribution with very few defects of larger thickness (Figure 5B). We attribute these differences to the drying dynamics of the film. Observations of the film during deposition showed that, in the evaporation regime, the complete drying of the film takes a longer time because of the presence of the meniscus in its vicinity. (The film is completely dried at a typical distance from the meniscus of approximately 500 μm .) This time may enable the film to reach a stable state before the complete evaporation of the solvent. Because the specific surface area per molecule depends on the presence of solvent, the film shrinks at the end of the drying process. If no reorganization is possible between layers of phospholipids, then this leads to the formation of holes. By increasing the solvent concentration in the atmosphere surrounding the dried film, we observed that holes were progressively closing until their complete disappearance, which is in agreement with the suggested mechanism.

All observations described above have been obtained using *n*-octane as a solvent, which is the total wetting situation on silicon. We found that when using a solvent under partial wetting conditions (e.g., chloroform) no deposition was obtained in the evaporation regime. Under the conditions of total wetting, instabilities can be observed under specific conditions. At low phospholipid concentration (<10 mg/mL) or high temperature (≥ 30 °C), the contact line of the meniscus becomes unstable, and a striped pattern parallel to the contact line is formed (Figure S2 in Supporting Information). This phenomenon is similar to

that observed with polymer solutions.^{7,18} At low temperature (i.e., significantly lower than ambient temperature), the film thickness becomes very inhomogeneous and abnormally large. This can be explained by the condensation of water from ambient air to the meniscus, as observed by Malaquin et al.¹⁹

Conclusions

We have experimentally and theoretically studied the situation of a confined, evaporating meniscus moving on a substrate at a constant speed and depositing a film of solute. Two regimes were identified depending on the relative importance of evaporation and viscous forces. In both cases, the film thickness is strongly dependent on the receding speed v and meniscus height d . This was applied to obtain multilayered phospholipid films with a thickness in the range of 20–200 nm and bilayer resolution (± 5 nm). This method to prepare dried phospholipid films in air opens new perspectives for studies on supported bilayer membranes,^{2,20,21} the preparation of well-defined liposomes,¹⁷ the controlled deposition of thin films,¹⁵ and biosensor technologies.^{3,22}

Acknowledgment. This work was partially supported by the ICORP 2006 “Spatio-Temporal Order” project (Japan Science and Technology Agency), Centre National de la Recherche Scientifique (CNRS), and the European Commission through project contract CP-FP 214566-2 (Nanoscales). M.L.B. received a grant from the EADS Foundation.

Supporting Information Available: Conversion of fluorescence microscopy images to thickness maps. Film instabilities. This material is available free of charge via the Internet at <http://pubs.acs.org>.

LA803646E

(18) Xu, J.; Xia, J.; Hong, S. W.; Lin, Z.; Qiu, F.; Yang, Y. *Phys. Rev. Lett.* **2006**, *96*, 066104.

(19) Malaquin, L.; Kraus, T.; Schmid, H.; Delamar, E.; Wolf, H. *Langmuir* **2007**, *23*, 11513–11521.

(20) Albertorio, F.; Chapa, V. A.; Chen, X.; Diaz, A. J.; Cremer, P. S. *J. Am. Chem. Soc.* **2007**, *129*, 10567–10574.

(21) Harland, C. W.; Rabuka, D.; Bertozzi, C. R.; Parthasarathy, R. *Biophys. J.* **2008**, *94*, 4718–4724.

(22) Majd, S.; Mayer, M. *Angew. Chem., Int. Ed.* **2005**, *44*, 6697–6700.